Ultrafast All-Optical Coupling of Light to Surface Plasmon Polaritons on Plain Metal Surfaces

Nir Rotenberg,* Markus Betz, and Henry M. van Driel

Department of Physics and Institute for Optical Sciences, University of Toronto, Toronto, Ontario, M5S 1A7 Canada

(Received 14 December 2009; revised manuscript received 25 March 2010; published 29 June 2010)

We propose and demonstrate an ultrafast all-optical method to couple light to surface plasmon polaritons on planar gold films. By interfering two 150 fs, 810 nm pulses we excite a transient grating in the temperature of the free electrons of the metal, resulting in a grating in the dielectric function, and leading to a 1 ps launch window for plasmonic excitation. We use pump-probe experiments to identify these ultrashort plasmonic excitations between 520 and 570 nm.

DOI: 10.1103/PhysRevLett.105.017402 PACS numbers: 78.68.+m, 73.20.Mf, 78.20.N−, 78.47.J−

Collective electronic excitations bound to a metallic surface and propagating along an interface with a dielectric media play a key role in a vast array of scientific activity, ranging from physics and material science to biology [1,2]. Referred to as surface plasmon polaritons (SPP) and known for their sensitivity to the optical properties of the bounding materials as well as their intrinsic subwavelength field confinement, these optical modes are integral to developments in biochemical sensing and nanophotonics. It is usually assumed that the generation of these modes requires an external structure to overcome the momentum mismatch between the wave vector of the SPP on an unstructured metal surface and that of light in a vacuum; for such coupling on a metallic film the momentum transfer is generally achieved with a periodic structure such as a grating [3] or a prism in the Kretschmann configuration [4], while an optical fiber is typically used to end-fire couple light to a plasmonic waveguide [5]. These approaches, however, rely on permanent, bulky structures and can be rather restrictive in terms of their usable beam geometry.

In this Letter we propose and experimentally demonstrate a nonlinear optical method to directly launch SPPs onto planar metal surfaces. The method takes advantage of an effective momentum transfer between optical beams that is typical of four-wave mixing type experiments, though in our case the method is effectively a cascade of linear effects. Specifically, two noncollinear near-infrared femtosecond pulses simultaneously impinge on the metal establishing, through linear absorption, a transient grating of the free-electron temperature. Since this thermal grating results in a periodic modulation of the optical constants of the metal, it can provide the momentum necessary to couple light to the SPP modes on the otherwise unstructured metal film. We experimentally demonstrate this method for thin gold films utilizing the resonant enhancement of the photoinduced modifications to the dielectric response near the *d*-band resonance. We find the SPP launch window to be as short as 1 ps, pointing towards possible uses in high-frequency applications. Although the demonstration is on gold, this method is very general and is applicable to SPPs on both metals [6] and doped semiconductors [7] over a broad spectral range. Further, utilizing other mechanisms, such as free-carrier dispersion or molecular transitions, this method can be used to launch SPPs in a metal-semiconductor [8] or metal-organic [9] interface, though typically with longer switching times.

For our experiments we use a 50 nm film of gold, evaporated onto a microscope slide, since this limits electronic heat diffusion, resulting in higher peak electron temperatures. However, 50 nm is more than twice the SPP skin depth in the visible, ensuring an effective decoupling of the plasmonic modes of the two interfaces [10]. We focus two 150 fs (FWHM), 810 nm pulses from a 250 kHz Ti:sapphire amplified laser to a 200 μm spot (FWHM) and interfere them on the surface of the gold film; the peak pump intensities are $I_1 = 5.3\ \mathrm{GW\,cm^{-2}}$ and $I_2 = 7.5\ \mathrm{GW\,cm^{-2}}$.

By interfering the two pump beams we optically generate an absorption and index of refraction grating [inset to Fig. 1(a)]. The interference of the two copolarized pump beams results in an intensity profile on the surface of the sample,

$$I(x,t) = I_1(t) + I_2(t) + 2\sqrt{I_1(t)I_2(t)}\cos\left(\frac{2\pi}{\Lambda}x\right), \quad (1)$$

where $I_{1(2)}(t)$ is the time-dependent intensity of the first (second) pump beam, x is the displacement along the surface of the film, and Λ, the period of the modulation is

$$\Lambda = \frac{\lambda}{\sin\theta_1 + \sin\theta_2}. \quad (2)$$

Here, λ is the wavelength of the pump beams in a vacuum, and $\theta_{1(2)}$ are the angles of the pump beams as shown in the inset to Fig. 1(a). For our experiments, $\theta_1 \sim 43°$ and $\theta_2 \sim 2°$, such that $\Lambda \sim 1200$ nm.

The physics of the grating is explained as follows: The absorption of the periodic intensity results in a transient, spatially periodic distribution of the temperature of the free electrons in the gold film. The formalism describing the thermalization of the electrons is developed in Refs. [11,12]; this is a two-step process where energy is initially transferred from the incident photons to the free electrons which then thermalize on a time scale of ~500 fs due to electron-electron collisions [12,13]. In Fig. 1(b) we

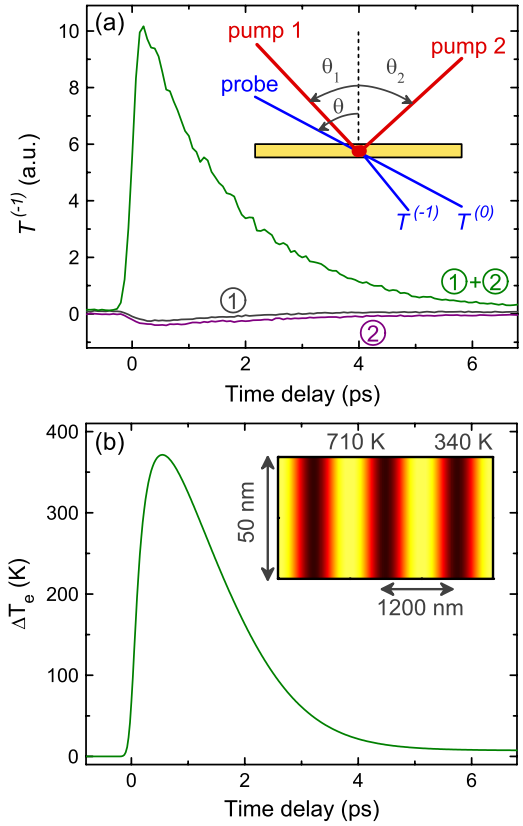

FIG. 1 (color online). (a) Time-dependent first order transmitted intensity when only one pump beam is incident (1 or 2), and when both pumps are simultaneously incident on the sample. The inset shows the experimental geometry including pump angles and the diffracted beam that is measured, $T^{(-1)}$. (b) The electron temperature contrast for the optically induced grating as a function of time delay between the pumps and the probe pulse. The inset shows the depth profile of the thermal grating on the sample at the time of peak changes, ~550 fs after overlap.

show the calculated difference in electronic temperature between the hot and cool regions of the gold film, as a function of time, while the inset represents the sample at ~550 fs after overlap, when the highest temperature contrast is achieved. We perform these calculations with the experimental parameters given above.

The change in electronic temperature manifests itself as a change of the distribution function, as electron states below the Fermi level are vacated and those above are filled; for gold, this distribution is centered about the *d*-band transition resonance, at 2.38 eV (520 nm). Since, for a given photon energy, the number of possible transitions is changed, an elevated electronic temperature ultimately results in a change to the real and imaginary parts of the dielectric function of the metal [14]. Thus, our pumping geometry leads to both an absorption and an index of refraction grating.

We confirm the presence of a grating as follows: From conservation of momentum calculations, in the plane of the film, we obtain the angles at which the diffracted orders propagate; we measure the intensity of light present in the first order diffraction in transmission, $T^{(-1)}$ [Fig. 1(a)], from a 200 fs (FWHM), 520 nm probe pulse. When only one of the two pump beams is incident on the sample only a small amount of light, which is scattered from the transmitted beam, arrives at the detector. However, if both beams are simultaneously overlapped on the sample, a large diffracted signal is clearly evident. From both the experimental trace, as well as the theoretical calculations, we extract a time constant of 1.0 ps for the decay of the grating.

The diffraction efficiency of such a grating is [15]

$$\eta = \left(\frac{\pi L}{\lambda}\right)^2 [(\Delta n)^2 + (\Delta \kappa)^2] e^{-\alpha L} \tag{3}$$

for a sample of thickness L, with an absorption coefficient α, and an induced change to the real and imaginary parts of the index of refraction, Δn and $\Delta \kappa$, respectively; here, $\eta = T^{(-1)}/I_0$ where I_0 is the incident probe intensity. As the thermally induced changes to the optical properties of the gold film are strongly wavelength dependent, decreasing in magnitude with the spectral distance separation from the *d*-band resonance at 520 nm [12,14], so too will the diffraction efficiency vary spectrally. In Fig. 2(a) we show the transient diffraction efficiency spectra predicted by Eq. (3) for a thermal grating theoretically generated using the same parameters as in the experiment.

We probe the grating and excite the SPPs with a broadband (450–750 nm) continuum, generated in sapphire. The continuum is focused to a 150 μm spot (FWHM) on the gold film and overlaps in time with the pumps. We then pass $T^{(-1)}$ through a monochromator coupled to a photomultiplier tube; the resulting spectra, with 2 nm resolution, are normalized to the back reflection from the half-wave plate that is used to control the polarization of the probe. The control over the polarization is crucial to this experiment, as the excitation of a SPP mode requires that the incident light have an electric field component in the direction of the propagation of the SPP [3]. Consequently, it is only a *p*-polarized probe pulse that can excite a SPP, and it is the difference between the *p*- and *s*-polarized probe signals that allows us to identify the plasmonic resonances. We measure $T^{(-1)}$ and not $T^{(0)}$ because the changes to $T^{(0)}$ due to the elevated electronic temperature can be on the order of several percent [16] and consequently can mask the energy lost to diffraction from the grating, while in the diffracted order we are only sensitive to grating effects.

A typical transient of the *p*-polarized first order transmission ($T_p^{(-1)}$) spectra is shown in Fig. 2(b), and is in good agreement with the expected diffraction efficiency shown in (a). The absolute diffraction efficiency, measured at 520 nm where the diffraction is the strongest, is $\sim 5 \times 10^{-4}$, becoming $\sim 1 \times 10^{-4}$ at 540 nm and $\sim 1 \times 10^{-5}$ at 570 nm; the absolute efficiencies predicted by Eq. (3) are 6.8×10^{-4}, 2.4×10^{-4}, and 4.7×10^{-5} at the same wavelengths, in very good agreement with the experimental

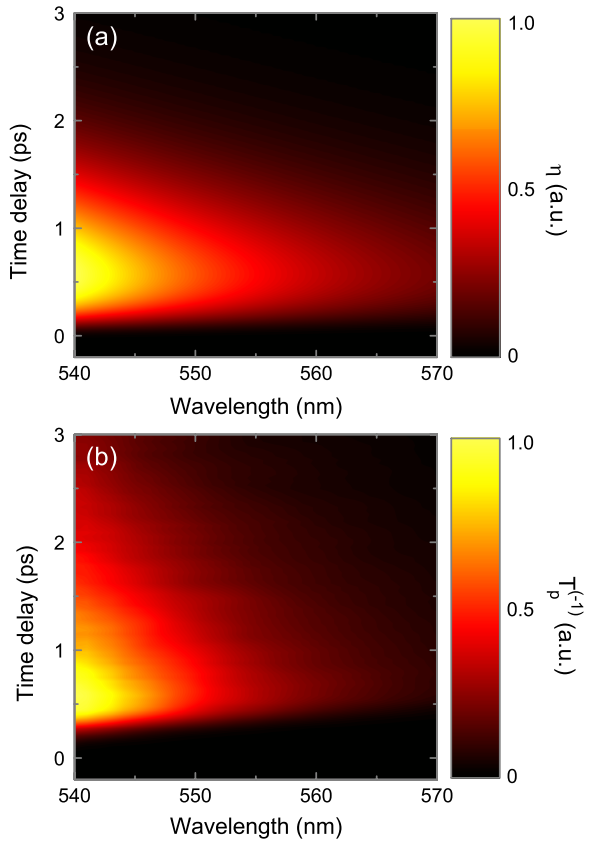

FIG. 2 (color online). First order diffraction efficiency from a thermally induced grating. (a) Theoretical diffraction efficiency transient between 540 and 570 nm. (b) Experimentally measured transient of the first diffracted order in transmission over the same range of wavelengths.

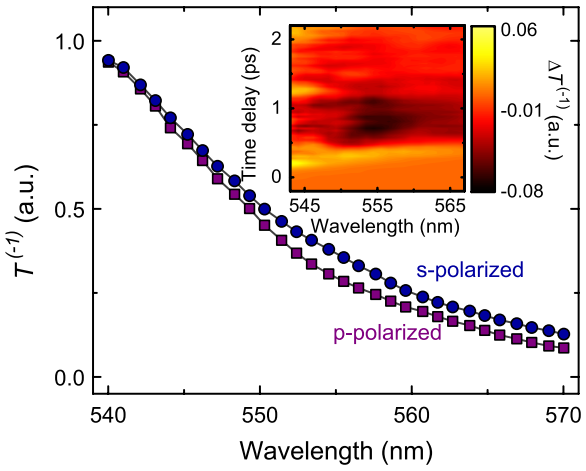

FIG. 3 (color online). p- and s-polarized $T^{(-1)}$ spectra 600 fs after overlap, at the time of highest grating contrast. The inset shows the transient of the difference between the two polarizations, with the plasmonic resonance revealed as the dark region in the center.

results. For both the experimental results, as well as the theoretical predictions, the grating decays with a time constant of ~1 ps, as the grating is washed out due to diffusion and as the electrons lose their energy to the gold lattice through electron-phonon scattering [12]; this, then, is the ultrashort window during which SPPs can be launched. Further, this ultrafast mechanism helps prevent reradiation of the SPP, as both the coupling and decoupling efficiencies are dependent on the presence of a grating.

To identify the plasmonic feature in $T^{(-1)}$ we compare p- and s-polarized spectra. In Fig. 3 we show both $T_p^{(-1)}$ and $T_s^{(-1)}$ at the time of peak thermal changes. Near the center of the plot, at ~555 nm, the difference between $T_p^{(-1)}$ and $T_s^{(-1)}$ is increased, as energy that would otherwise have been transmitted from the p-polarized probe is coupled to a SPP mode. This is more evident in the inset where we show the transient of this difference, $\Delta T^{(-1)} = T_p^{(-1)} - T_s^{(-1)}$, as a function of wavelength, and the plasmonic dip is recognizable by the dark region near the center; it is also evident that this feature decays in ~1 ps. Further, at the peak of $\Delta T^{(-1)}$ about 8% of the light that would have been diffracted into this order is coupled to a SPP. Taken together with the absolute diffraction efficiencies given above, we calculate a plasmonic coupling efficiency of 10^{-5}, which, given the relative mode confinements results in a ratio of peak plasmonic to incident radiation intensities of 10^{-2}. However, given that most of the light is contained in the zero-order transmission and reflection, it is reasonable to assume that the total coupling efficiency is much greater than we show; indeed, finite-difference time-domain (FDTD) simulations predict a coupling efficiency of 10^{-2}, when all the diffraction orders are considered, although corresponding experiments must be performed for verification.

The plasmonic resonance is easier to identify by considering a single $T_p^{(-1)} - T_s^{(-1)}$ spectra at the peak of the grating diffraction, as is done in Fig. 4; here, we show different resonances corresponding to different excitation angles, θ, ranging from 37.5° to 44.5°. By rotating the sample we change the angle of incidence of the probe continuum, changing the component of the momentum of the incident light that is in the plane of the gold film. From momentum conservation we then expect the plasmonic resonance to shift according to [3]

$$k_{\mathrm{SP}} = k_0 \sin\theta + m k_G, \tag{4}$$

where k_{SP} is the SPP wave vector, $k_0 = 2\pi/\lambda$ is the free-space wave vector, $k_G = 2\pi/\Lambda$ is the grating wave vector, and m is an integer. In the inset to Fig. 4 we show both the measured, as well as the calculated spectra shifts to the SPP resonance due to a change in θ, for $m = 1$; that is, it is not the slowly varying difference between $T_p^{(-1)}$ and $T_s^{(-1)}$ but rather the sharp spectral feature that shifts according to Eq. (4) that we regard as the signature of plasmonic coupling. The three resonances shown in the main figure are circled.

Spectrally tuning the plasmonic resonance allows us to explore the limitations of the optically induced transient

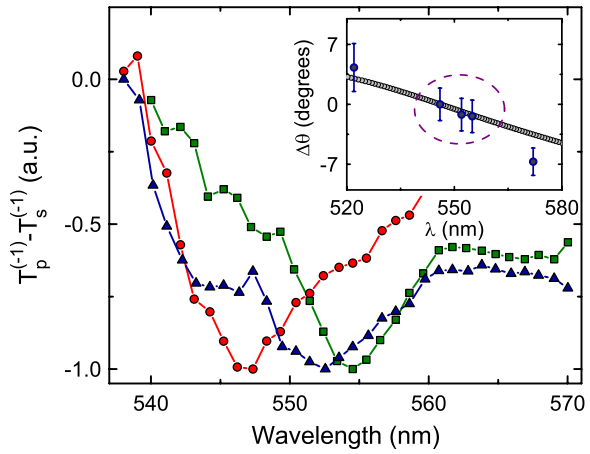

FIG. 4 (color online). $\Delta T^{(-1)}$ spectra at the time of peak grating diffraction for different excitation geometries show different plasmonic resonances. The inset shows the measured spectral displacement of the resonances vs the change in incident angle (points), as well as the theoretically expected behavior (line).

free-electron temperature grating coupling. While the three resonances near 550 nm have dips that are in the same order of magnitude, the dips of the other two resonances shown in the inset of Fig. 4 are much smaller. As we expect, the longer wavelength resonance near 570 nm is smaller in amplitude than those at 550 nm by a factor of $\sim$40; this is due to the large spectral separation from the *d*-band resonance at 520 nm and the consequent small changes to the density of states at these wavelengths, and hence to a small induced Δn and $\Delta \kappa$. More surprising, the resonance near 520 nm is also $\sim$10 times smaller in amplitude than those near 550 nm even though it occurs near the peak of the induced changes to the optical properties of the gold. We suggest that this occurs because of the proximity of the *d*-band resonance which provides another absorption channel.

To conclude, we propose and demonstrate a new ultrafast method to couple light to SPP modes on plain metal films. By interfering two 150 fs, near-infrared beams on the surface of a thin, unstructured gold film, we generate a transient grating in the free-electron temperature, and hence in the optical properties of the material. The grating decays with a time constant of $\sim$1 ps, allowing for an ultrashort launch window for SPPs before the system recovers. By varying the polarization of the probe beam, as well as the excitation geometry, we identify a polarization-dependent feature which spectrally shifts in the correct manner for a SPP resonance. In essence, our method allows for plasmonic coupling without the need for external structures such as gratings or prisms. Since the submission of this manuscript we have become aware of a related scheme for coupling light to surface plasmons on flat metal surfaces [17]. Here, Renger *et al.* employ a nonresonant nonlinear effect achieving a ratio of peak plasmon intensity to peak incident intensity that is 7 orders of magnitude smaller than is observed with the resonant scheme described here.

This method of all-optical coupling of light to SPPs can be generalized and might be appropriate for on-chip plasmonic circuits, where waveguide modes could be used to generate the grating and couple to a SPP. It could also be employed with, for example, a metal-semiconductor interface in which an optically induced free-carrier density grating could be used to couple infrared light to an SPP over a much larger bandwidth than given here. Overall, optically induced transient gratings could be used to excite SPPs on unstructured metallic films with ultrafast time scales, an exciting combination for future plasmonic based nanophotonic devices.

We gratefully thank Jan N. Caspers for his help with the data acquisition, Tak Sato for his assistance with the sample fabrication, and Mohamed Swillam for the FDTD simulations. We acknowledge funding provided by the Natural Sciences and Engineering Research Council of Canada.

*nrotenbe@physics.utoronto.ca

[1] W. L. Barnes, A. Dereux, and T. W. Ebbesen, Nature (London) **424**, 824 (2003).
[2] J. A. Schuller, E. S. Barnard, W. Cai, Y. C. Jun, J. S. White, and M. L. Brongersma, Nature Mater. **9**, 193 (2010).
[3] H. Raether, *Surface Plasmons*, edited by G. Hohler (Springer, Berlin, 1988).
[4] E. Kretschmann and H. Raether, Z. Naturforsch. A **23**, 2135 (1968).
[5] G. I. Stegeman, R. F. Wallis, and A. A. Maradudin, Opt. Lett. **8**, 386 (1983).
[6] K. F. MacDonald, Z. L. Sámson, M. I. Stockman, and N. I. Zheludev, Nat. Photon. **3**, 55 (2009).
[7] A. K. Azad, H.-T. Chen, S. R. Kasarla, A. J. Taylor, Z. Tian, X. Lu, W. Zhang, H. Lu, A. C. Gossard, and J. F. O'hara, Appl. Phys. Lett. **95**, 011105 (2009).
[8] E. Hendry, M. J. Lockyear, J. Gómez Rivas, L. Kuipers, and M. Bonn, Phys. Rev. B **75**, 235305 (2007).
[9] R. A. Pala, K. T. Shimizu, N. A. Melosh, and M. L. Brongersma, Nano Lett. **8**, 1506 (2008).
[10] J. A. Dionne, L. A. Sweatlock, H. A. Atwater, and A. Polman, Phys. Rev. B **72**, 075405 (2005).
[11] S. I. Anisimov, B. L. Kapeliovich, and T. L. Perel'man, Zh. Eksp. Teor. Fiz. **66**, 776 (1974); [Sov. Phys. JETP **39**, 375 (1974)].
[12] C.-K. Sun, F. Vallée, L. H. Acioli, E. P. Ippen, and J. G. Fujimoto, Phys. Rev. B **50**, 15337 (1994).
[13] R. H. M. Groeneveld, R. Sprik, and A. Lagendijk, Phys. Rev. B **51**, 11433 (1995).
[14] R. Rosei, F. Antonangeli, and U. M. Grassano, Surf. Sci. **37**, 689 (1973).
[15] H. J. Eichler, *Laser-Induced Dynamic Gratings* (Springer, New York, 1986).
[16] N. Rotenberg, A. D. Bristow, M. Pfeiffer, M. Betz, and H. M. van Driel, Phys. Rev. B **75**, 155426 (2007).
[17] J. Renger, R. Quidant, N. van Hulst, S. Palomba, and L. Novotny, Phys. Rev. Lett. **103**, 266802 (2009).